Absolute Electron Analyzer

Keisuke Goto

Nagoya Institute of Technology, Gokiso-cho, Showa-ku, Nagoya 466-8555, Japan

kgoto@system.nitech.ac.jp

(Received: Mar 2, 2002)

Absolute energy calibration method in an Auger electron spectroscopy (AES) has been developed, which is a self-consistent method in our novel cylindrical mirror energy analyzer (CMA). Detail characteristics of the CMA were studies and the calculable properties were confirmed. Elastically backscattered primary electrons of constant energy distribution for the calibration range associated with a precision primary voltages (SI traceable) were used as a reference standard and an iteration method was applied. The obtained results are the kinetic energies of referenced to the vacuum level of the CMA, in which the thermionic emissions and the work functions of the cathode and the CMA are automatically corrected. Feasibility of 15-meV(σ) of the energy calibration for the kinetic energies referencing on the vacuum level ranging 10eV through 1200eV was shown. The work function of the sample was corrected respecting to the CMA by measurements an onset of the secondary electron characteristics by changing the sample bias.

Keywords: Absolute energy calibration, Iteration method, Elastically backscattered primary electrons, Energy analyzer, CMA, Work function, Secondary electrons.

1. Introduction

Standard class of energy calibration in AES and XPS should be based on the SI traceable method with a calculable energy analyzer, which is a metrology of absolute measurements. Thought it has not ever been achieved, as no reasonable standards and correction method for the contact potential (work function) had been established. Historically, the endeavors have been the calculable analyzers with energy, length, voltage, and magnetic strength, but little with contact potential. The first great work of absolute measurements was made by Thomson [1] employed all of the available methods in an absolute way to measure the energy. It should be noticeable that he had mentioned that the "moving electrons seem likely to be heavier in mass than at rest" even in 1897. It was before Einstein (1905). The other scientists also mentioning about it. Robinson and Rawlinson [2] improved the 180° - type magnetic analyzer [3] and examined the Plank's relation of $E=h\nu$ *i.e.*, XPS, which is now used as a standard[4]. They observed the energy obtained at far edge of the spectra, which is now called the Fermi edge and related it to the x-ray energies. Though the exact relation between the wave length of the x-rays and the electron energy of the Fermi edge has still been uncertain in high accuracy[5]. Ellis[6] published quite accurate absolute energy values for γ-rays by using a similar analyzer[2,3]. More recently Siegbahn[7] made quite accurate experiments with an elaborate apparatuses after Ellis[8], in which some known characteristic x-ray energies were used as calibration standards, *i.e.*, the differences between the spectra not the Fermi edge. While Anderson and Lee[5] employed field emitted electrons and a standard voltage to assess the Fermi edge of Ni and obtained the uncertainty of 60meV. Miller *et.al.*,[9] also studied the uncertainty in the Fermi edge detection with a particular energy resolution in an actual energy analyzer and obtained quite material dependent results due to the asymmetric edge structures. An approximate correction for the x-rays to the photoelectron energies was given by Keski-Rahkonen[10], which is a simple calculation.

Another standard for the energy calibration may be a "voltage" in **SI** units, because we commonly use "voltage" in the acceleration of thermal or field emitted electrons in AES. The thermal electrons (thermionic) have been conventionally used in the energy (kinetic) calibration of AES. The accuracy of this method, however, would be 0.5–1eV on account of the energy distribution of the emitted electrons from the actual electron gun and the work functions of the constituent parts. The electron gun that is a kind of high and/or band pass energy filter will modify the original energy distribution, thus the energy distributions discussed by Young[11] are not

always applicable. Bearden and Schwarts[12] and Beardn *et.al.*,[13] used well defined thermionic emissions and observed the x-rays to obtain ***h/e*** values. Powell *et.al.*,[14] calibrated the AES and XPS in an accuracy ±0.2~ ±0.4eV by using a thermionic emission and a standard voltage, in which they assumed the effective work function of the cathode and the most probable energy to be ***kT***. Lassetre *et.al.*,[15] calibrated the energy analyzer by using two known spectra as standards. *i.e.,* the difference method like as Siegbahn[7]. We have briefly surveyed these works[16].

We would like to conclude that the energy calibration by using a thermionic emission that is a source to excite Auger electrons is quite a practical and accurate method but with some proper implementations; well defined thermionic emissions and standard voltage. The elastically backscattered primary electrons (**BE**) from the sample have been used as the thermionic emission with corrections[17,18].

Correction for the work function is a next significant remaining problem, which has not been completed until now. It is necessary in a kinetic energy calibration to get a reference vacuum level. The work function was discussed as a contact potential by Kelvin in 1898[19], referring to the venerable Volta's experiments of 95 years before then! His technique of a "quadrant" electrometer with ideally high-impedance and the results were excellent, though performed in the atmosphere. In an actual analysis, the measurements of the work functions of both the analyzer and the sample are impractical. But we need the actual *in situ* values. We will introduce a method to correct the difference in work functions by observing an onset of secondary electrons from the sample[20].

2. Experiments

Thermionic emission of the electron gun

We chose a CMA as a candidate for the standard. It has great advantages over other analyzers; calculable in design, excellent efficiency, and almost symmetric transfer function. The last feature is plausible for the peak determination, which CHA don't have[7]. A novel prototype CMA[21] of almost calculable ($\Delta E/E = 0.25\%$) has been used with some improvements. The basic designs[22,23] have been given and quite a similar CMA with us also been calculated[24]. The experimental arrangement is shown schematically in Fig.1. The CMA has two gaps at both ends with center radii r_g of

$$r_g = 1/4(r_a + r_b + \sqrt{r_a \cdot r_b}). \quad (1)$$

The ghost spectra (scattered electrons in the CMA) were reduced from 0.15-0.2% to below 0.01% with an additional slit (not shown) to cut the extraneous electrons[25] after the Monte Carlo simulation[26]. The surfaces that would be hit by any electrons are coated with soot and/or aquadag to reduce the electrons scattering and to obtain a uniform work function. A new electron gun with a particular tungsten hairpin cathode, which provides unipotential[12,13] and reduced magnetic field properties for the well defined thermionic emissions. The thermionic cathode is a modified tungsten hairpin type with a ball like cathode consisting of a few grains of diameter 0.3mm on the top of the hairpin of diameter 0.127mm. The potential drop and magnetic field on the cathode surface are about 2.5% and 20% of the conventional type, respectively. The characteristics were simulated by using model made of a glass enveloped as large as 100 times and mercury in it. The temperature difference at the top of the cathode and the shank being as small as 5K can be observed. The cathode was normally operated at about 2050K. This electron gun was not considered to be the finest focus but a well defined stable energy distribution of the thermionic emission. The electron gun provides an "extractor" operated at V_e of typically 80V with respect to the cathode to get a constant energy distribution of the thermionic emission and this characteristic might be preserved irrespective of the final accelerating voltages. Thus below the 80V of acceleration the *e*-gun was operated in the retarding mode with poor focusing property. The beam diameters were typically 0.22mm for 1000V and 0.48mm for 100V of E_p's being assessed by the edge of a Faraday cup (a kind of knife edge method). These diameters were comparable or larger than the detection slit of the CMA of about 0.183mm. It should be preferable that the beam diameters were a factor of smaller than that of the slit. The i_p was measured with the Faraday cup of diameter 1.7mm bored through the sample holder. A part of the sample holder is made of quartz tube to reduce the thermal expansion due to the sample heating by the primary electron beam, since 1-μm of the relative expansion is affective. An

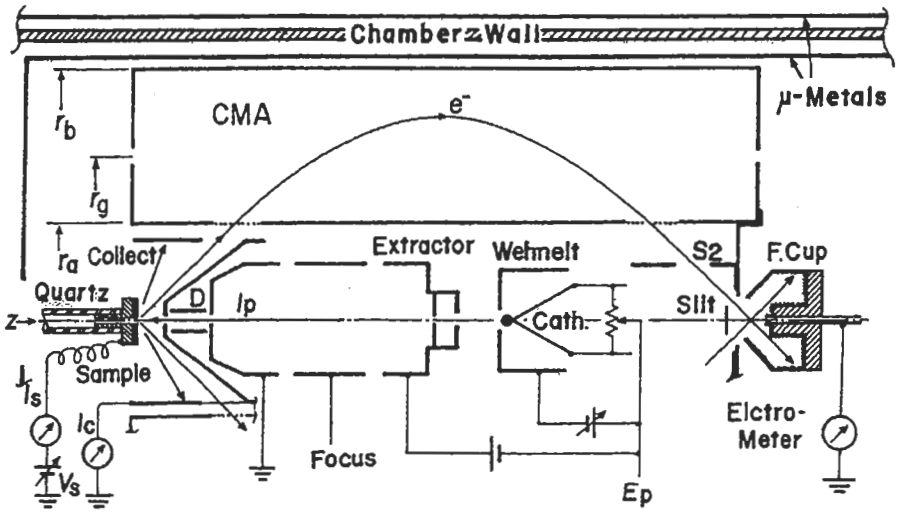

Fig.1. Schematic experimental arrangement.

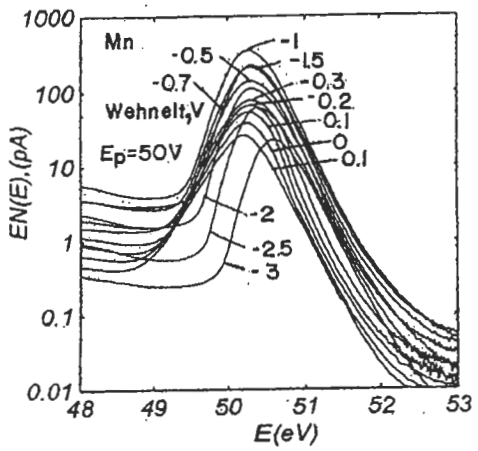

Fig.2. Thermionic emission: E_p=50V, Wehnelt bias, +0.1~-3V.

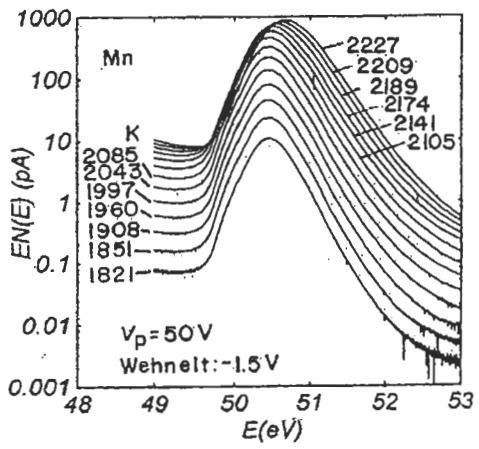

Fig.3. Thermionic emission: E_p=50V, T=1821~2227K.

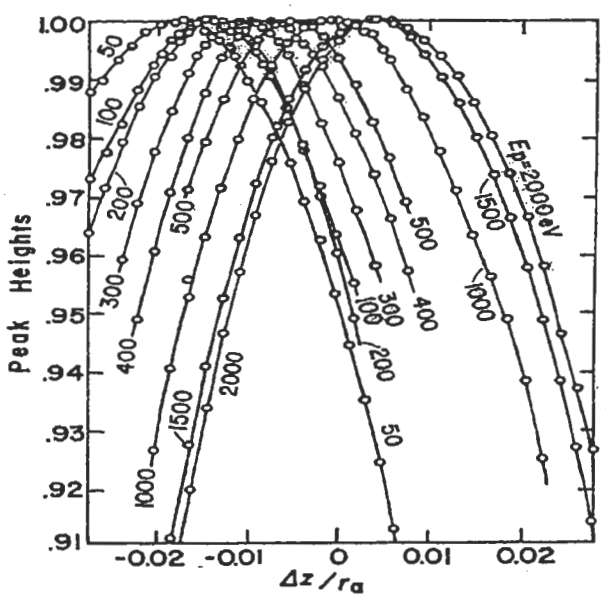

Fig.4. Peak heights of the elastically backscattered primary electron (BE), E_p=50~2000eV, as a function of sample position.

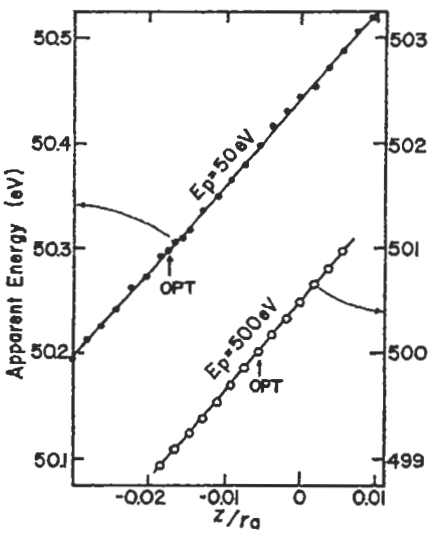

Fig.5. Linearity of the CMA as a function of the sample position for E_p's of 100eV and 1000eV.

experimenter is one of the greatest external heat sources as well. The heat radiated from the experimenter near the chamber should considerably warm the apparatus and room. This was appreciable in the experiments. The change of i_p for E_p's higher than 40V(cut-off energy) to 3kV was 4% and this might be caused by the focusing and vignetting properties in the *e*-gun. Gradual decrease of i_p for lower than 40V of E_p's down to 10V might not be due to the space charge because the decrease was far slower than 3/2 power law but to the vignetting at the apertures of the broadened beam as a result of Coulomb repulsion in the e-gun. The emission stability was typically 0.1% for 2-hour and 0.01% for 10-min *i.e.*, 0.01 of the standard deviation in Gaussian distribution at the top can be detected. This characteristic was very important in the present study to determine the top position of the spectrum precisely.

The residual magnetic field in the CMA was far below 1mG (detection limit of a F.W.Bell model 620), thus it is capable of measuring slow secondary electrons as low as 1eV. The sample can be biased, V_s, through a tri-axial arrangement. The energy spectra were measured using an electrometer (Keithley model 642LN) with a Faraday cup. To calibrate the electronics, we have provided standards; voltages of Fluke 731B and 732B, voltage divider of Fluke 752A, resistors of Fluke of Fluke 742A, esi SR-1 series, Alfa Electronics ASR series, DMM of HP-3458A, Keithley 2001, and 2002, pA-source of Keithley 261.

The thermionic emissions obtained, the **BE** from Mn (incidentally being set), for E_p of 50V in a semi-log plot are shown in Fig.2. Almost true energy distribution can be obtained in this low E_p since the effects of energy resolution of the CMA being relatively small. The Wehnelt bias were +0.1V through -3.0V for the constant temperature 2054K. The Wehnelt bias should change not only the peak intensity by a factor of 15 but also energy position by 0.33eV. It seems that the Wehnelt bias would determine the cut-off energy. Farther, the onset of the emission also shifted by about 0.83eV. The on-set should rise at "vacuum" level of the cathode for the low Wehnelt bias, though it shifted too low energies for +0.1V. This might arise probably from the broadened beam on account of the too large cross-over just before the Wehnelt. Thus the theory[11] would be of no use however the work function of the cathode might be known. On the contrary, the same terms were also examined for the constant Wehnelt bias (-1.5V) by changing the cathode temperature 1821K through 2227k, though the changes were about the order of kT [11] or less until the effect of space charge would appear, Fig. 3. Thus we can introduce an *iteration* method to determine the peak position irrespective of the work functions. We operated the cathode at the Wehnelt bias of about -1V and the energy distribution might have been kept unchanged throughout the experiments. A coaxial (with CMA) ion gun (shower like) with a shutter to keep the CMA clean was set outside the CMA far left in the figure (not shown).

Peak intensities *vs* sample positions: Relativistic effects

The relativistic effects[10,18] which was briefly described so early as in 1897 by Thomson[1], can be seen in electrostatic analyzers as a shift of energy, sample positions, and intensities on account of the travelling velocities. We have confirmed these effects[27] and new details are shown in Fig. 4. It shows peak intensities of **BE** in heights as a function of the sample position z along the axis of the CMA (normalized by the diameter r_a of the inner cylinder with plus direction being into the CMA), being referenced for the optimum sample position for the E_p of 1000V. There exists only one optimum position for each E_p on account of the relativistic focussing properties. This characteristic is quite discernible from the magnetic analyzers[28] as the all electrons travelling in the magnetic analyzer do not receive any change of their momentum in the analyzer. Each characteristic curve seems to be a universal curve of CMA except for these in the lower energies, *i.e.*, below 200 eV. The relativistic effects shall not be so effective in the lower energies as 500 eV, but the shift of the optimum position does not cease. This can be considered as the consequence of the broadened primary beams and the angular distribution of the **BE**, though the analysis is very difficult. The apparent energy as a function of the sample position for far separate two E_p's (100- and 1000-V of acceleration; conventionally in eV) is shown in Fig. 5. The experimental points correspond simultaneously to these in Fig.4. It should be noted that two curves

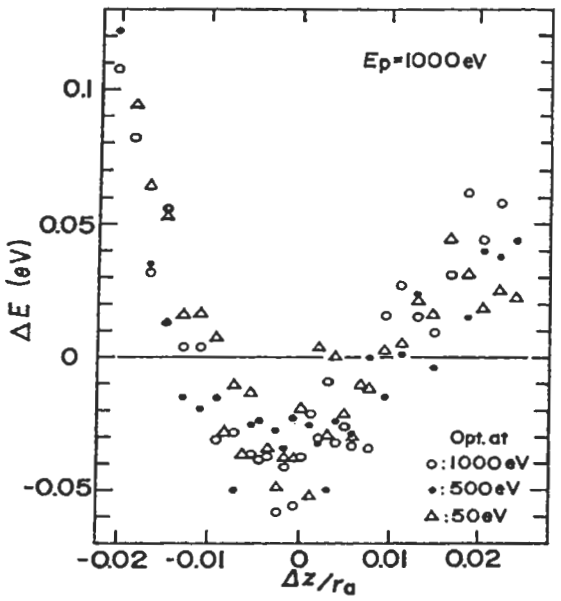

Fig.6. The linearity error of Fig.5 for E_p=1000eV.

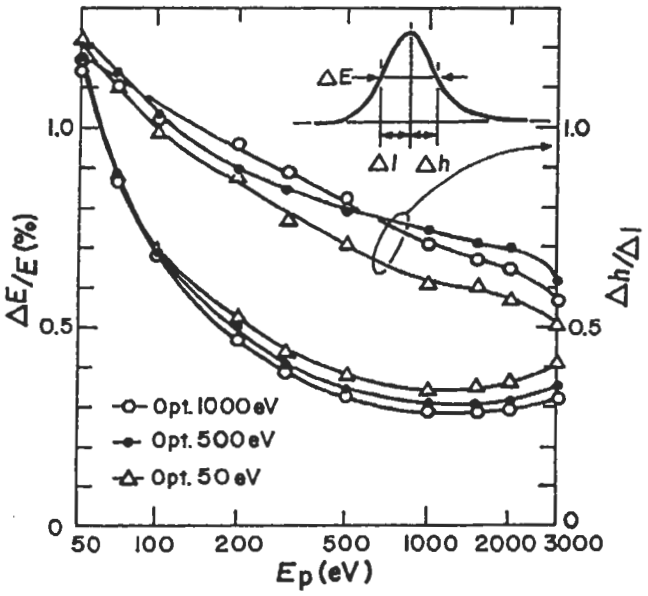

Fig.7. Energy resolution and asymmetric features of the BE for three optimized positions.

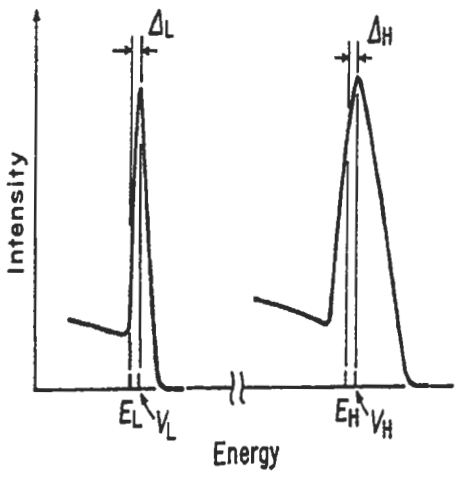

Fig.8. Schematic energy calibration; iteration method.

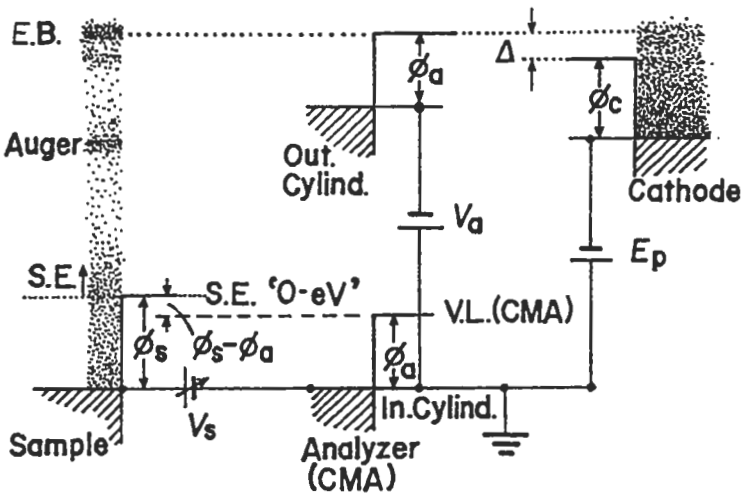

Fig.9. Schematic energy calibration.

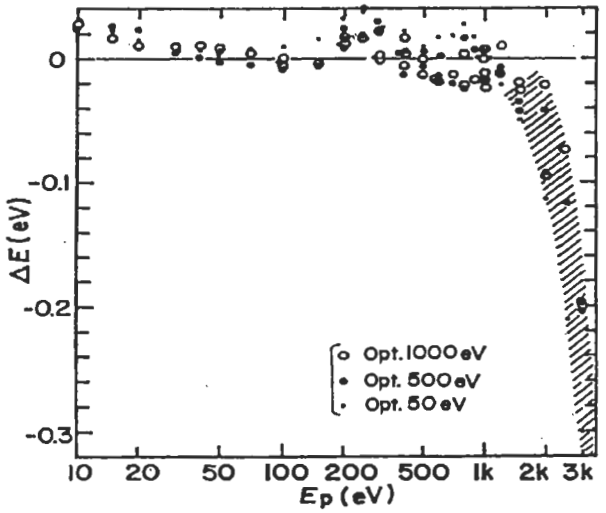

Fig.10. Energy calibration by the iterative method.

seem quite straight and parallel with each other, even though the optimum positions are different. This is a focusing property of CMA. These characteristics would make us to convince an energy calibration to be feasible. The linearities are 0.9995 and 0.9998 for the acceleration voltage E_p's of 100V and 1000V, respectively. The linearity error for the curve of 1000V is shown in Fig. 6, as a departure ΔE from the straight line. This characteristic determines the ultimate obtainable error in the calibration.

The observed energy resolution FWHM, ΔE / E (%), and asymmetric features, Δ_h / Δ_l, at the optimized sample positions for E_p's of 1000V, 500V, and 50V are shown in Fig. 7. No corrections have been made on the data, such as for the spectra overlaps, the primary beam broadening, and the transfer characteristics of the CMA. The energy resolution was not so distinctive in the lower energies because the actual energy resolution is far smaller than the FWHM of the **BE**, It became, however, sensitive in the higher energies for the sample positions. The increases in the higher energy ends were accounted for the increased overlapping of the spectra, *i.e.*, **BE** and plasma losses, while the relativistic effects for the ΔE in these energy ranges would be of more minor ones. The asymmetric characteristics, which were rather complex, would mainly come from the transmission of the CMA, focusing property with sample position, and the overlaps of the spectra, see also Fig. 10. The sudden drops at the highest energy could be explained by the increased overlaps of the spectra. A PC simulation using experimental spectra presented quite identical features[2]. These changes of **BE**, *i.e.*, the asymmetry and energy resolution, might introduce considerable uncertainties in an absolute energy calibration[8]. Though it will be found in the following section that the asymmetry was not so serious.

Energy calibration by iterative method

A schematic energy calibration is shown in Fig. 8. We must work out a relation between the primary electron acceleration voltage of E_p's(given values) and applied voltages, V_a as V_H and V_L, on the analyzer by observing a spectrum of **BE** from the sample. The relation should be,

$$E=K(\Delta+V_a)+\delta, \qquad (2)$$

where the true kinetic energy is E, K a transfer coefficient of the CMA, Δ (unknown) the off-set energies arising from the actual thermionic emission, the work functions (cathode and CMA), and δ (unknown, but assumed to be zero) the residuals. If all terms are known then the energy calibration is very easy by using **BE** as standard, as similar as Siegbahn[7], Powell *et al.*,[14] and Lassettre *et.al*[15]. It cannot be possible, as shown in Fig.3, there should exist an uncertainity in the most probable thermionic emission on the Wehnelt bias even though the work function of the cathode is known. Here we introduce an iterative method, in which two separate primary acceleration voltages, for example, E_H=1000V and E_L=100V, will be used and Δ_H and Δ_L are assumed to be constant as Δ. We really observed the **BE** as follows. First, a coefficient K to transfer the applied voltage V_H of the analyzer and Δ to the energy E is presumably set for the higher E_H, say 1000V and 0.2eV, so as to be E_H=1000eV+0.2eV(~kT). This is a first approximation and approximate K can be obtained. Then the E is set to be 100V and E of 100.33 eV may be obtained. Second, the E_H 1000V will be set again and a new K value is set for E_a=1000+0.33=1000.33 (eV). Using this new K value, we measure E for E_L=100V and E=100.34 eV may be obtained. Third, the newest K value may be set for E_p=1000-v so as to obtain E_a=1000+0.34=1000.34 (eV). We will repeat these series of processes until the same values below decimal points are obtained (converged), say E=1000.35 eV and 100.35 eV and then the transfer coefficient K is finally determined. An ultimate scatter of the calibration should be determined by the characteristics in Figs. 5 and 6. The energy so determined is a self-consistent absolute kinetic energy based on the "*vacuum*" level of the analyzer. Because, if the V_a is presumable "zero-V" the corresponding electron of "zero eV" kinetic energy will pass through the CMA. The value has been automatically corrected for the work function of the cathode, actual thermionic emission energy E_{th}, and unbalance of the heating circuit of the cathode in Fig. 1. This is schematically shown in Fig. 9. In this calibration, the corrections for the relativity[18] and the recoil losses[19] were included, however, those for the overlaps of the spectra (following section) and the work function of the sample were presently not included.

The K and Δ can easily be obtained by simple

calculation as,

$$K=(E_H-E_L)/(V_H-V_L), \quad (3)$$

$$\Delta=1/2(E_H-E_L)(V_H+V_L)/(V_H-V_L)-1/2(E_H-E_L). \quad (4)$$

But the iteration is realistic, as it will converge in some uncertainty.

In Fig. 10 the obtained results are shown, in which the sample positions were optimized for E_p=50V, 500V, and 1000V with corresponding transfer coefficient K's being 1.49918, 1.49688, and 1.49533, respectively. Theoretical[21,22] non-relativistic K value is 1.495 for our particular CMA with a ratio of the radii of the outer- to inter-cylinder of the CMA being 2.4 (±0.2%). The errors ΔE by referencing precise voltage E_p for the energy range 10 eV through 1200 eV scattered rather randomly with a standard deviation of 15 meV. This would show that any optimized position (~±0.02 of $\Delta z/r_a$) can be used in the calibration with particular transfer coefficient. The characteristics rapidly dropped for the energy higher than 1200 eV, the shaded area, can be explained by the increased overlap of the spectra due to the poor energy resolution of the CMA. This convolution effect will be briefly shown below. On the other hand, the systematic errors in the lowest energies might be raised from the $EN(E)$ property of the CMA as the actual energy window of the CMA is far smaller than the energy width of the BE, thus the higher energy components were enhanced.

Work function correction by secondary electrons

As can be seen in Fig. 9, the work function is a key term in energy calibration, because it determines the reference level of the "*vacuum*" zero. It has been granted that work function and secondary (SE) have close relation. One of the characteristics of SE, we will use, is that its energy distribution begins at 0eV of the vacuum level in the sample. No evident criticism on this consideration is found, however, we have tacitly believed so.

Total spectra

A log-log plot that covers the whole range of energy distribution including Auger spectra in one sheet is shown in Fig. 11. We call it as "advanced Sickafus plot" [29] for E_p of 5keV. This plot is quite convenient in general use. It should be noted that the spectra ranging 0.1~ 10 eV showed the work function difference, interband transitions, and structures due to the plasmon excitation [30] in the true secondary electron range.

Nominal workfunctions are ~5eV for C/graphite, 4.3eV for Al, 4.7eV for Cu, 4.3eV for Ag, 5.7eV for Pt [31]. The almost flat characteristics in the range 0.1-1 eV are consisted of the rubbish electrons, *i.e.,* background, in the CMA [25]. One of the reasons that the curves do not consist with at the onset of the true **SE** is apparently due to the work function difference. Particularly, the sudden deflection observed in Pt just above 1 eV is caused by the acceleration of **SE** to the CMA by the work function difference, as the relative work function of the sample Pt is the largest.

By changing sample bias (V_s) from –1.0 V to 1.0 V in every 0.1 V for E_p=50 V, we obtained the energy distribution of **SE** from Mn of slightly oxidized but stable. It is shown in Fig. 14. Fig. 14 reveals the relationship between the onset of **SE** and the sample bias voltage. In the bottom section, with the sample bias decreasing from 1.0 V to –1.0 V, the $EN(E)$ simultaneously becomes less at the same kinetic energy. While in the top section it is contrary. It is because the energy distribution of true **SE** was artificially shifted with respect to the CMA and subjected to the window characteristics as $EN(E)$. Thus the deceleration and the acceleration could occur and the intermediate stage should exist between the two extremes. The intermediate stage would necessarily be the stage of the "0" of the work function difference. We urged to find this "0-stage".

To find the "0-stage", the bottom of Fig. 14, the almost the onset parts of SE are displayed in Fig.15. The characteristics begin to concentrate at V_s of about -0.1V~-0.2V, *i.e.,* the border between the modes of acceleration (coarse) and the deceleration (fine) for the SE by the retarding potentials. This critical voltage should correspond to the relative work function of the sample to CMA being null and can be used to correct the work function difference. We appreciated the correction can be a vicinity of –0.1V through –0.2V. This method is totally self-consistent.

3. Summary

It has been proved that the energy calibration of tens meV in AES by using elastically backscattered

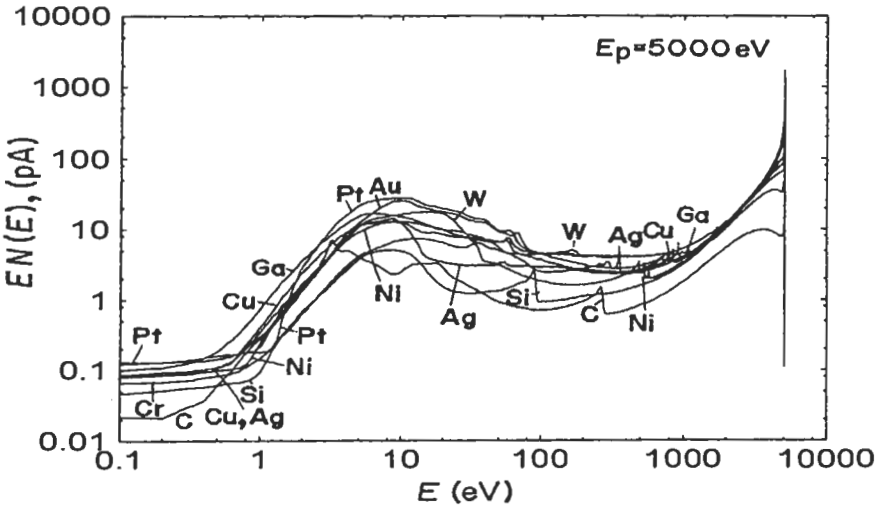

Fig.11. Total spectra in "log-log" plot for typical elements, for E_p=5000eV.

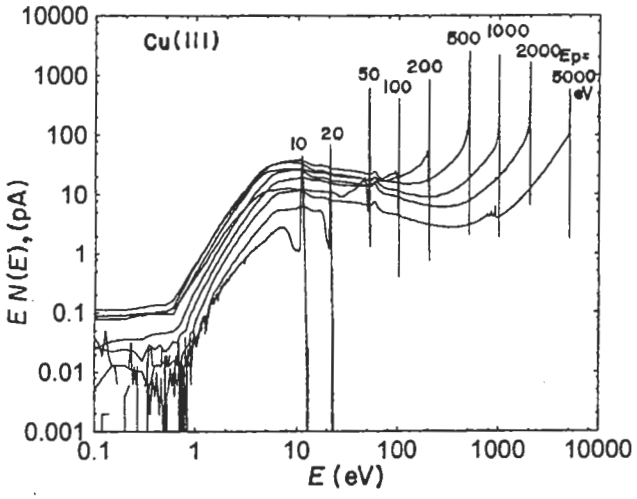

Fig.12 Total spectra from Cu(111) for E_p=10ev~5KeV.

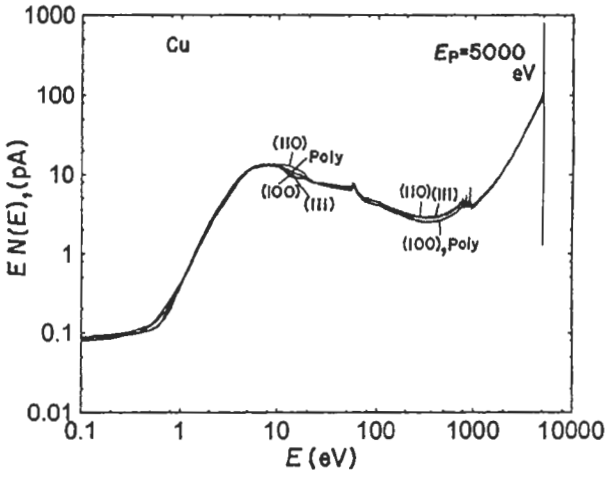

Fig.13 Total spectra from Cu(100),(110),(111), for E_p=5KeV

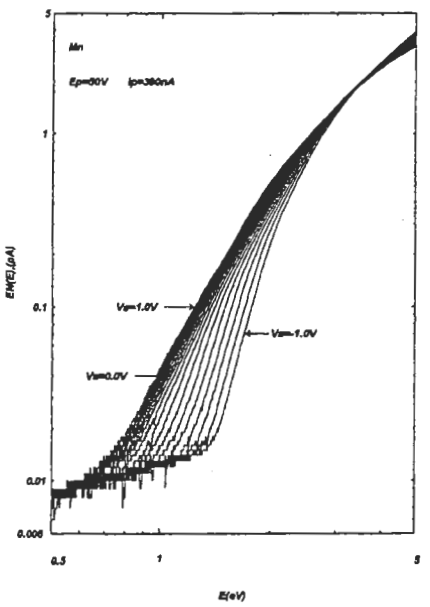

Fig.14 True SE spectra, onset, as a function of the sample bias.

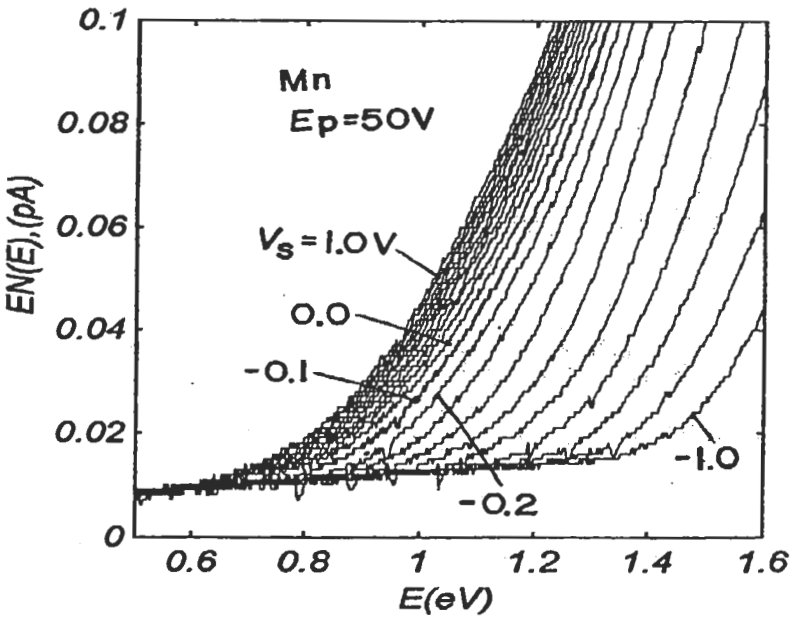

Fig.15 The magnified characteristic of Fig.14, around onset.

primary electrons can be feasible with an iterative method, which is automatically corrected for the energy position of the apparent thermionic emission of the electron gun. This calibration is referenced to the vacuum zero level of the analyzer (CMA) and self-consistent. The standard in this method is a voltage E_p being **SI** traceable. The correction for the relative work functions of the sample and the analyzer was made by the careful measurements of the onset characteristics of the secondary electrons. This is also a self-consistent correction in the absolute calibration. It was found that by combining the two methods the complete absolute kinetic energy calibration can be made.

Acknowledgement

I would like to sincere thanks to Prof. R.Shimizu of Osaka Institute of Technology, Dr.M.P.Seah of NPL, C.J.Powell of NIST, Professor L.Kövér of ATOMKI, Dr. J.Tòth of ATOMKI for their helpful comments and encouragements. Members of SASJ and JSPS Committe 141-Microbeam Analysis have continuously encouraged us. Techinical assisstance of Mr.M. Iwafune, Mr.S.Sakakibara, Mr.K.Fujii, and Mr.Y.Z.Jiang (my student) should be addressed. This work has been supported by the aid of the Special Coordinated Research of Science and Technology through NRIM and the fund from NMC.

References

[1] J.J.Thomson, Phil. Mag. **44**, 293 (1897).
[2] H.Robinson and W.F.Rawlinson, Phil. Mag. **28**, 277 (1914).
[3] E.Rutherford and H.Robinson, Phil.Mag, **26**,717 (1913).
[4] M.T.Anthony and M.P.Seah. Surf. Interface Anal. **6**, 95 (1984).
[5] C. R. Anderson and R.N.Lee, J. Electron Spectrosc. Relat. Phenom. **34**, 173 (1984).
[6] C.D.Ellis, Proc. Roy. Soc. London, **A143**, 350 (1934).
[7] K. Siegbahn, Ark. Mat. Astr. Fys.**30A** (No.20), (1944).
[8] C.D. Ellis, Proc. Roy. Soc. London, **A139**, 336 (1933).
[9] A.C.Miller, C.J.Powell, U.Gelius, and c.R. Anderson, Surf. Interface Anal. **26**, 606 (1998).
[10] O.Keski-Rahkonen and M.O.Klause, J.Electron Spectrosc. Relat. Phenom. **13**, 107 (1978).
[11] R.D.Young, Phys.Rev. **113**, 110 (1959).
[12] J.A.Bearden and G.Schwartz, Phys. Rev. **79**, 674 (1950).
[13] J.A Bearden and F.T.Johnson, and H.M. Watts, Phys. Rev. **81**,70 (1951).
[14] C.J. Powell, N.E.Erickson, and T.Jach, J.Vac. Sci. Technol. **20**, 625 (1982).
[15] E.N. Lassetre, A.Skerbele, M.A. Dillon, and K.J.Ross, J. Chem. Phys. **48**, 5066 (1968).
[16] K.Goto, N.Nissa Rahman, Y.Z.Jiang, Y.Asano, and R.Shimizu, Surf. Interface Anal. (to be published).
[17] H.Boersch, R.Wolter, and H.Schoenebeck, Z.Phys. **199**, 124(1967).
[18] O.Keski-Rahkonen, J.Electron Spectrosc. Relat. Phenom. **13**, 113(1978).
[19] Lord Kelvin, Phil. Mag. **46**, 82(1898).
[20] Y.Z.Jiang, W.L.Li, K.Goto, and R.Shimizu, J. Surface Anal. (to be published).
[21] K.Goto, N. Sakakibara, and Y.Sakai, Microbeam Anal. **2**, 123(1993).
[22] V.V.Zashkvara, M. I. Korsunski, and O. S. Kosmachev, Sov. Phys.-Tech. Phys. **11**, 96 (1996).
[23] H.Z. Sar-El, Rev. Sci. Instrum. **38**, 1210(1967); **41**, 561(1970).
[24] D.Varga, Á.Kövér, L.Kövér, and L.Redler, Nuc. Instrum. Meth. Phys. Res. **A238**, 393 (1985).
[25] N.Nissa Rahman, K.Goto, and R.Shimizu, J.Surface Anal. **8**, 2 (2001).
[26] M.M.El Gomati and T.A.El Bakush, Surf. Interface Anal. **24**, 152(1996).
[27] K.Goto and R.Shimizu, *ALC'97,* 403-406 (Maui, Hawaii, 23-28 Nov. 1997).
[28] E.Persico and C. Geoffria, Rev. Sci. Instrum. **21**, 945 (1950).
[29] Y.Z.Jiang, K.Goto, and R.Shimizu, J. Surface Anal. **8**, 147 (2001).
[30] F.Pellerin, et. al., Surface Sci. **103**, 510 (1981).
[31] R.W.Strayer, W.Mackie and L.W.Swanson, Surface Sci. **34**, 225 (1973).